Article

The Neighboring Component Effect in a Tristable [2]Rotaxane

Yuping Wang, Tao Cheng, Junling Sun, Zhichang Liu,
Marco Frasconi, William A. Goddard, and J. Fraser Stoddart

Just Accepted

1
2
3
4
5
6
7
8
9
10
11
12
13
14
15
16
17
18
19
20
21
22
23
24
25
26
27
28
29
30
31
32
33
34
35
36
37
38
39
40
41
42
43
44
45
46
47
48
49
50
51
52
53
54
55
56
57
58
59
60

The Neighboring Component Effect in a Tristable [2]Rotaxane

Yuping Wang,[†] Tao Cheng,[‡] Junling Sun,[†] Zhichang Liu,[∇] Marco Frasconi,[§]

William A. Goddard III,[‡] and J. Fraser Stoddart*,[†,⊥,∥]

[†]*Department of Chemistry, Northwestern University, 2145 Sheridan Road, Evanston, Illinois 60208, USA*
[‡]*Materials and Process Simulation Center, California Institute of Technology, 1200 East California Boulevard, Pasadena, California 91125, USA*
[∇]*School of Science, Westlake University, 18 Shilongshan Road, Hangzhou 310024, China*
[§]*Department of Chemical Sciences, University of Padova, Via Marzolo 1, Padova 35131, Italy.*
[⊥]*Institute for Molecular Design and Synthesis, Tianjin University, 92 Weijin Road, Nankai District, Tianjin 300072, P.R. China*
[∥]*School of Chemistry, University of New South Wales, Sydney, NSW 2052, Australia*

*E-mail: stoddart@northwestern.edu

MAIN TEXT

*Correspondence Address
Professor J Fraser Stoddart
Department of Chemistry
Northwestern University
2145 Sheridan Road
Evanston, IL 60208-3113 (USA)
Tel: (+1)-847-491-3793
E-Mail: *stoddart@northwestern.edu*

Abstract: The redox properties of cyclobis(paraquat-*p*-phenylene) cyclophane (CBPQT^{4+}) renders it a uniquely variable source of recognition in the context of mechanically interlocked molecules, through aromatic donor-acceptor interactions in its fully oxidized state (CPBQT^{4+}) and radical-pairing interactions in its partially reduced state (CBPQT$^{2(\bullet+)}$). Although it is expected that the fully reduced neutral state (CBPQT$^{(0)}$) might behave as a π-donating recognition unit, resulting in a dramatic change in its binding properties when compared with the other two redox states, its role in rotaxanes has not yet been investigated. To address this challenge, we report herein the synthesis of a tristable [2]rotaxane in which a CBPQT^{4+} ring is mechanically interlocked with a dumbbell component containing five recognition sites—(i) one, a bipyridinium radical cation (BIPY$^{(\bullet+)}$) located centrally along the axis of the dumbbell, straddled by (ii) two tetrafluorophenylene units linked to (iii) two triazole rings. In addition to the selective recognition between (iv) the CBPQT^{4+} ring and the triazole units, and (v) the CBPQT$^{2(\bullet+)}$ ring and the reduced BIPY$^{(\bullet+)}$ unit in the dumbbell component, investigations in solution have now confirmed the presence of additional noncovalent bonding interactions between the CBPQT$^{(0)}$ ring, acting as a donor in its neutral state towards the two tetrafluorophenylene acceptors in the dumbbell component. The unveiling of this piece of molecular recognition in a [2]rotaxane is reminiscent of the existence in much simpler, covalently linked, organic molecules of neighboring group participation (anchimeric assistance giving way to transannular interactions) in small-, medium-, and large-membered rings.

Introduction

The neighboring group effect,[1-2] alias anchimeric assistance, occupies a special place in the annuls of physical organic chemistry and organic stereochemistry. The intramolecular nature of the effect which, not only leads to the speeding up of reactions[3-8] when they are potentially operative, but

also often dictates[9-11] regio- and stereospecifically the constitutions and configurations of the products obtained under tight stereochemical control in what are geometrically constrained environments. This intramolecular effect, which was explored in acyclic as well as cyclic molecules, is one of the keystones of what became known as conformational analysis.[12] Already back in 2012, we argued in a review[13] that the thermodynamic parameters associated with model host-guest complexes provide a good starting point to rationalize the ratio of ground-state and metastable co-conformations in bistable[2]rotaxanes at equilibrium. We demonstrated that these [2]rotaxanes exhibit a strong correlation between their ground-state distribution constants and the relative free energies of closely related model complexes. We pointed out in the review that the semiquantitative treatment of the ground-state distribution of co-conformations (translational isomers)[14] is reminiscent of the type of conformational analysis[12] that can be carried out on multiply substituted cyclohexane rings once the conformational free energies—also referred to as A-values[12]—between equatorial and axial substituents on monosubstituted cyclohexane rings are known. Although caution has to be exercised in applying the principle[12] of the additivity of A-values, the approach is generally one that can be used in a predictive manner. Now, let us assume that we introduce into a rotaxane, a recognition site between the ring and dumbbell components that is known to be an extremely weak one, at least in the context of a host-guest complex.[15] Will we witness an intramolecular neighboring component effect in the rotaxane that is analogous to the neighboring group effect in molecules that only contain covalent bonds?

Recently, we reported[16] that, although a 1:1 inclusion complex between the fully reduced π-electron-rich cyclobis(paraquet-p-phenylene) (CBPQT$^{(0)}$) ring and the π-electron-deficient guest 1,4-dicyanobenzene (DCB) can be isolated as a solid-state superstructure, the binding constant for this host-guest complex in (toluene) solution is too small to be measured by the usual techniques.

Now, what if this 1:1 host-guest complex was to be transplanted, so to speak, into a rotaxane, would the DCB unit constitute a recognition site for the $CBPQT^{(0)}$ ring? In this paper, we set out to answer this question by designing a tristable [2]rotaxane, which (i) allows us to explore the interactions of the $CBPQT^{(0)}$ ring with recognition sites that reflects the electronic properties of DCB and, at the same time, (ii) makes it possible for us to understand more about the CBPQT ring in its different redox states, i.e., $CBPQT^{(0)}$, $CBPQT^{2(\bullet+)}$ and $CBPQT^{4+}$ interacting with three different recognition sites on the dumbbell component—namely, π-electron-deficient, radical and π-electron-rich sites, respectively—which have been chosen for incorporation into the dumbbell component of a tristable [2]rotaxane. A bipyridinium ($BIPY^{2+}$) unit was introduced into the dumbbell as the radical recognition site thanks to the well-established[17-20] recognition between the $CBPQT^{2(\bullet+)}$ ring and the bipyridinium radical cation ($BIPY^{\bullet+}$). By contrast, the choice of the π-electron-rich recognition sites for $CBPQT^{4+}$ is subtle, since the ideal candidate should be able to interact with the $CBPQT^{4+}$ ring, while not competing with the desire of the π-electron-rich $CBPQT^{(0)}$ to interact with the π-electron-deficient recognition sites on the dumbbell component. In order to meet these two requirements, we have introduced triazole units which act (i) as the π-electron-rich recognition sites for $CBPQT^{4+}$ and, at the same time, (ii) as the means of templating the synthesis of the tristable [2]rotaxane by the copper(I) catalyzed azide-alkyne cycloaddition[21] (CuAAC). Finally, for the π-electron-deficient sites, tetrafluorinated phenylene (Ar^F) units are introduced[16] in the knowledge that the changes in the chemical environments of these Ar^F units can be monitored by ^{19}F NMR spectroscopy, an additional tool which would provide us with clear-cut evidence for the location of the ring component in both the fully oxidized and neutral states. Based on these considerations, we report (Scheme 1a) herein a tristable [2]rotaxane, where the $CBPQT^{4+}$ ring is mechanically interlocked with a dumbbell component containing $BIPY^{2+}$,

triazole and Ar^F units. By performing experiments at different redox potentials on this [2]rotaxane, any interactions between the $CBPQT^{(0)}$ ring and the π-electron-deficient Ar^F units in solution will be revealed. We show, by (i) ^1H and ^{19}F NMR spectroscopies, (ii) UV/Vis/NIR spectroscopy, (iii) cyclic voltammetry (CV) studies and (iv) DFT-based calculation that the different redox states of the ring interact with different recognition sites on the dumbbell component, demonstrating that this tristable [2]rotaxane can serve as a multi-state molecular switch.[22]

Results and Discussion

Synthetic Protocols. The *para*-substituted tetrafluorophenylene building block **3**, which was prepared according to literature procedures,[23] was subjected (Scheme 1b) to bromination, nucleophilic substitution with 4,4'-bipyridine and counterion exchange (NH_4PF_6 / H_2O) in order to afford the viologen-based precursor **5•2PF$_6$** in an overall yield of 60 %. While the radical and the π-electron-deficient sites are already incorporated into $\mathbf{5}^{2+}$, the formation of the triazole unit was achieved along with the formation of the [2]rotaxane, **1•6PF$_6$**, in the presence of the **CBPQT**$^{4+}$ ring and the alkyne-functionalized stopper precursor **6**, by employing (Scheme 1b) a Cu-mediated synthetic methodology in a threading-followed-by-stoppering protocol developed recently by us.[21] Briefly, the azide-functionalized, dumbbell precursor **5•2PF$_6$** and **CBPQT•4PF$_6$** were dissolved in MeCN in a 1:1 molar ratio under an atmosphere of Ar, followed by the addition of an excess of Cu^0 dust (diam < 425 μm). Upon stirring the reaction mixture for 20 min, the $BIPY^{2+}$ units in both $\mathbf{5}^{2+}$ and **CBPQT**$^{4+}$ are reduced by Cu^0 to their corresponding radical cationic states, and the solution turns dark purple on account of the formation of the inclusion complex $\mathbf{5}^{•+} \subset \textbf{CBPQT}^{2(•+)}$. Cu^I ions are generated *in situ* during this process, allowing the CuAAC reaction to take place and generate the [2]rotaxane following the addition of the alkyne-functionalized stopper precursor **6**

to the reaction mixture. The dumbbell **2**•2PF$_6$ was also prepared (Scheme 1b) in order to serve as a reference. Compounds **1**•6PF$_6$ and **2**•2PF$_6$ were purified by column chromatography and counterion exchange (NH$_4$PF$_6$ / H$_2$O). The characterization of the compounds was carried out by high-resolution electrospray ionization mass spectrometry (HR-ESI-MS) and by both ^{1}H and ^{13}C NMR spectroscopies. See the Supporting Information for detailed synthetic procedures and characterizations.

Fully oxidized states. With both the dumbbell and the [2]rotaxane in hand, we investigated their properties in their fully oxidized states by performing ^{1}H and ^{1}H–^{1}H COSY NMR experiments. In comparison (Figure 1b) with the ^{1}H NMR spectrum of the structurally symmetric **2**•2PF$_6$, that of **1**•6PF$_6$ displays a more complicated spectrum (Figure 1b) as a consequence of the presence of the ring component, shuttling along the dumbbell component slowly on the ^{1}H NMR timescale. Since the CBPQT^{4+} ring is located (Figure 1a) on one portion (*vide infra*) of the dumbbell component, it has little effect on the chemical shift of one set of protons, e.g., protons *a* and *b*, etc. As a result, these protons have similar chemical shifts to those observed in the case of the dumbbell **2**•2PF$_6$. On the other hand, their counterparts, such as protons *a′*, *b′* and *c′*, experience significant changes in chemical shift on account of their being much closer to the ring component. These chemical shifts define the location of the CBPQT^{4+} ring. Indeed, amongst all these shifts, that of the triazole proton ($H_{TR}′$) experience the most significant changes in chemical shift (Figure 1b) in an upfield direction by almost 5 ppm, i.e., from 8.36 to 3.72 ppm, compared with its counterpart (H_{TR}). This observation suggests that the shielding region of the CBPQT^{4+} ring, located inside the ring cavity as a result of aromatic ring currents,[24] has the profound influence upon one of the two triazole protons. By contrast, the signals for both proton *a′* and $H_α′$ are shifted downfield. In addition, the

^{19}F NMR spectrum of **1**•6PF$_6$ reveals that the signals for $F_a{}'$ and $F_b{}'$ are also downfield-shifted, compared with those of F_a and F_b, respectively. This observation confirms unambiguously the hypothesis that, in the fully oxidized state, the CBPQT^{4+} ring encircles preferentially the relatively π-electron-rich triazole unit rather than the π-electron-deficient Ar^F units. It is also noteworthy that, while the shuttling motion of the CBPQT^{4+} ring along the dumbbell component is often observed[24] in analogous viologen-based [2]rotaxanes, variable-temperature (VT) ^{1}H and ^{19}F NMR spectra of **1**•6PF$_6$ show that the two sets of the peaks for the protons and ^{19}F nuclei on the dumbbell component do not undergo coalescence within the temperature range from 233 to 343 K, an observation which indicates that shuttling does not occur on the NMR timescale. See SI, Section 5. Indeed, the limiting chemical shifts for the slowly exchanging methylene protons a' (6.21 ppm) and a (6.16 ppm) at 343 K allows an estimation[25] of the energy barrier which is greater than 17.5 kcal mol^{-1}. This observation is rationalized by the fact that in addition to the Coulombic repulsion arising from the centrally located BIPY^{2+} unit on the dumbbell component, the introduction of the π-electron-deficient Ar^F units into the dumbbell component presumably further increases the energy barrier, preventing the CBPQT^{4+} ring from shuttling.

Radical cationic states

In order to understand the molecular behavior of the [2]rotaxane in its radical state, cyclic voltammetry (CV) was performed on **1**$^{6+}$ and **2**$^{2+}$. Upon scanning the potential in the negative direction, the dumbbell **2**$^{2+}$ undergoes (Figure 2a) a single-electron reduction process at –244 mV, generating the radical state **2**$^{•+}$. This potential, which is significantly higher than that[17] (–460 mV) of the analogous viologen-based compounds having no Ar^F rings, is ascribed to the fact that the BIPY^{2+} unit in **2**$^{2+}$ raises its propensity to receive an electron because of the adjacent electron-withdrawing Ar^F rings. In comparison, the highly positively charged [2]rotaxane **1**$^{6+}$ is more prone

to receive electrons: the reduction process occurs in a stepwise manner. In the first instance, it takes up (Figure 2b) two electrons at –143 mV—with one going[18, 24] to the $BIPY^{2+}$ unit in the dumbbell component and the other going to one of the two $BIPY^{2+}$ units in $CBPQT^{4+}$—to generate a bisradical tetracationic species $\mathbf{1}^{2+2(\bullet+)}$, an intermediate which is stabilized by the pimerization between the two reduced $BIPY^{\bullet+}$ radical cations. Subsequently, a single electron reduction of the other $BIPY^{2+}$ unit in $CBPQT^{2+(\bullet+)}$ at –217 mV leads to formation of the trisradical tricationic state $\mathbf{1}^{3(\bullet+)}$. The anodically shifted reduction potential of this overall three-electron reduction process, in comparison with those of other [2]rotaxanes[17, 24] containing $CBPQT^{4+}$ encircling a $BIPY^{2+}$ based dumbbell, can also be ascribed to the electron-withdrawing effect of the Ar^F rings. Following an addition of an excess of Zn dust to the MeCN solution (100 μM) of $\mathbf{1}^{6+}$ and $\mathbf{2}^{2+}$, respectively, the radical cationic states of the [2]rotaxane and the dumbbell were probed by UV/Vis/NIR spectroscopy. See SI, Section 6. The spectrum of the dumbbell $\mathbf{2}^{\bullet+}$ displays absorption bands at wavelengths around 400 and 605 nm, both peaks characteristic[26] of the $BIPY^{\bullet+}$ radical species. The lack of the NIR absorption indicates that the intermolecular radical-pairing interaction between two dumbbell molecules is very weak at 100 μM. On the other hand, an absorption band center on 1091 nm—evidence for the formation of the trisradical tricationic species—is observed in the case of the [2]rotaxane $\mathbf{1}^{3(\bullet+)}$, which is further confirmed (Figure S9c) as an intramolecular process with the assistance of concentration-dependent UV/Vis/NIR experiments. Thus, we conclude that, upon the reduction to its trisradical tricationic state $\mathbf{1}^{3(\bullet+)}$, the $CBPQT^{2(\bullet+)}$ ring encircles the $BIPY^{\bullet+}$ station on the dumbbell.

Neutral states

The recognition between $CBPQT^{(0)}$ and the Ar^F rings in the [2]rotaxane in its neutral form was investigated in detail. UV/Vis/NIR Spectroscopic investigations were performed on the neutral

[2]rotaxane and its dumbbell counterpart—namely $\mathbf{1}^{(0)}$ and $\mathbf{2}^{(0)}$—which can be generated[16] by titrating the strong chemical reductant cobaltocene (CoCp$_2$) into both MeCN solutions (50 μM) of $\mathbf{1}^{6+}$ and $\mathbf{2}^{2+}$, respectively, under an Ar atmosphere. Specifically, upon the addition of 1.0 equiv of CoCp$_2$ to the solution of $\mathbf{2}^{2+}$, the initial colorless solution (Figure 3a, blue trace) turns dark blue, displaying (Figure 3a, purple trace) similar absorption bands to those of the solution of $\mathbf{2}^{2+}$ treated with Zn dust, indicating the rapid formation of the radical state $\mathbf{2}^{\bullet+}$. After further addition of 5 equiv of CoCp$_2$ to this solution,[27] the reduction from $\mathbf{2}^{\bullet+}$ to $\mathbf{2}^{(0)}$ is confirmed by the disappearance of the radical absorption band (605 nm) and the concomitant increase of the absorption band at 371 nm, characteristic[16, 28-29] of the neutral BIPY$^{(0)}$ units (Figure 3a, red trace). A closer examination of the spectra of $\mathbf{2}^{(0)}$ revealed the presence of a weak absorption band at 520 nm—a feature that has not been observed in the previously reported BIPY$^{(0)}$-contained systems. The reduced forms of the of the [2]rotaxane were generated by titrating a solution of $\mathbf{1}^{6+}$ with CoCp$_2$ as well. The conversion of all three BIPY^{2+} units in $\mathbf{1}^{6+}$ to their radical cationic states was achieved (Figure 3b, purple trace) after the addition of 3 equiv of CoCp$_2$. The resulting spectrum is characterized by an absorption band at 1091 nm which corresponds to the formation of the trisradical tricationic species. This absorption band decreased in its intensity upon the further addition of 8 equiv of CoCp$_2$, resulting in a new set of peaks at 376 (Figure 3b, red trace) and 550 nm (Figure 3b-c, red trace) which indicate the generation of the neutral species $\mathbf{1}^{(0)}$. It should be noted that the absorption band at 550 nm has a much higher extinction coefficient when compared with that of the peak at 520 nm for $\mathbf{2}^{(0)}$.

Taking all these observations into account, we have hypothesized that both the absorption bands at 520 nm for $\mathbf{2}^{(0)}$ and 550 nm for $\mathbf{1}^{(0)}$ result from charge transfer interactions. In the case of $\mathbf{2}^{(0)}$, charge transfer process takes place (Figure 3d) intramolecularly between the neutral BIPY$^{(0)}$ and

the Ar^F units. See SI, Section 9. In contrast, rather than the Ar^F units interacting with the $BIPY^{(0)}$ unit on the dumbbell, the mechanically interlocked structure of $1^{(0)}$ allows the Ar^F units to interact (Figure 3d) with the neutral $CBPQT^{(0)}$ as a result of its being encircled by the ring. In this manner, charge transfer between the Ar^F unit and the two $BIPY^{(0)}$ units in the ring component can take place in a face-to-face manner, while the shuttling motion of the ring component along the dumbbell makes it possible for the ring to adopt the most optimized co-conformation so as to maximize these interactions. In other words, charge-transfer is facilitated in the case of $1^{(0)}$, giving rise to the significantly higher molar extinction coefficient as well as the 30 nm red-shifted absorption band on going from the neutral dumbbell to the neutral [2]rotaxane. By employing a different reduction protocol (see SI, Section 9), the absorption spectra of these neutral species were also measured in toluene, and shown to be consistent with the observations in MeCN.

The results from CV also help us gain an understanding of the interactions between the Ar^F rings and $CBPQT^{(0)}$ in the case of $1^{(0)}$. In analogous viologen-based [2]rotaxanes[24] without Ar^F rings, the reduction from the trisradical tricationic state to the neutral state occurs in a stepwise manner, wherein the formation of the bisradical dicationic intermediate—stabilized by radical-pairing interactions—can be observed. By contrast, the [2]rotaxane $1^{3(\bullet+)}$ undergoes (Figure 2b) a simultaneous three-electron reduction at -686 mV to generate $1^{(0)}$. This observation can be rationalized by the fact that, once one of the $BIPY^{\bullet+}$ units in $CBPQT^{2(\bullet+)}$ is reduced to the neutral state, the ring will move away from the radical recognition site as a result of the interactions between the Ar^F rings and the $BIPY^{(0)}$ unit, leading to the collapse of the bisradical dicationic intermediate so that all the $BIPY^{\bullet+}$ units are reduced simultaneously.

More evidence for the recognition between $CBPQT^{(0)}$ and the π-electron-deficient Ar^F rings were obtained from ^1H and ^{19}F NMR spectroscopies. Samples suitable for NMR experiments were prepared[16] (see SI, Section 7) by extracting the neutral species $\mathbf{1}^{(0)}$ and $\mathbf{2}^{(0)}$ from a biphasic system using $CD_3C_6D_5$ as the organic layer under an Ar atmosphere. By comparing the chemical shifts of the protons and fluorine nuclei in the dumbbell and [2]rotaxane, we can characterize the fully reduced [2]rotaxane and identify the recognition sites encircled by the $CBPQT^{(0)}$ ring in the neutral state. In the case of the dumbbell compound, the reduction from the fully oxidized state $\mathbf{2}^{2+}$ to the neutral state $\mathbf{2}^{(0)}$ leads to (Figure 4b) significant upfield chemical shifts of (i) the protons H_α and H_β on the $BIPY^{2+}$ unit, which resonate at 5.47 and 5.60 ppm, respectively, as well as (ii) a signal for the methylene protons a at around 3.55 ppm, revealing the loss of the aromaticity upon reduction of the $BIPY^{2+}$ unit. In the case of the neutral [2]rotaxane $\mathbf{1}^{(0)}$, the presence of a single species was confirmed (Figure S11) by diffusion-ordered ^1H NMR spectroscopy (DOSY), which afforded a diffusion coefficient of 8.2×10^{-10} m^2 s^{-1}, demonstrating that the mechanically interlocked structure is retained during reduction. All the proton resonances of $\mathbf{1}^{(0)}$ can be assigned with the assistance of ^1H–^1H NOESY spectroscopy. In particular, the peaks for $H_{\alpha1}$ and $H_{\beta1}$ on the $BIPY^{(0)}$ units in the $CBPQT^{(0)}$ ring appear, respectively, at 5.41 and 5.35 ppm (Figure 4c), values which are close to those reported[16] for the free neutral $CBPQT^{(0)}$. On the other hand, the ^{19}F NMR spectra help us pinpoint the location of the $CBPQT^{(0)}$ ring component in the neutral state. Notably, the fluorine nuclei resonances for the [2]rotaxane $\mathbf{1}^{(0)}$ are shifted (Figure 4c) upfield compared with those for the dumbbell $\mathbf{2}^{(0)}$, as a result of shielding by $CBPQT^{(0)}$ encircling one of the two Ar^F rings at any instant in time. In particular, the signal for F_b experiences an upfield shift of 2.34 ppm, which is greater than that (0.46 ppm) of F_a, indicating that F_b resides closer to the center of the cavity of $CBPQT^{(0)}$ than does F_a. It should also be noted that DNMR shows (see SI, Section 8)

only one set of peaks are observed for the protons and fluorine nuclei on the dumbbell component

in $\mathbf{1}^{(0)}$ over a range of temperature from 193 to 298 K, demonstrating that $CBPQT^{(0)}$ undergoes fast

shuttling on the NMR timescale along the dumbbell in the neutral state. In the absence of peak

separations, a maximal energy barrier of 9.6 kcal mol^{-1} for the shuttling can be estimated.[30] Since

shuttling of $CBPQT^{4+}$ is slow on the NMR timescale in the fully oxidized form of the [2]rotaxane

$\mathbf{1}^{6+}$, this redox-controllable energy barrier to shuttling paves the way to developing slide-ring-

based materials[31-32] with switchable properties. It should also be noted that the shuttling rate of the

ring at its neutral state can be modulated by varying the binding affinity between the recognition

sites and the ring, i.e., the higher the binding affinity, the lower the shuttling rate.

Computational Studies

We carried out DFT calculations on the level of M06-2X/6-311G**[33] with zero dumping D3

correction[34] as implemented in Jaguar 8.2[35] (more details can be found in SI) to characterize the

interactions of the CBPQT ring component with the [2]rotaxane in different charge states from its

fully oxidized (6+) to the neutral state (0) form. The inclusion of continuum solvent corrections in

the DFT is, however, not sufficient to capture the full effect of solvent and cations on the structures

and energetics, which becomes increasingly important in the case of higher charged states, i.e., the

radical and the fully oxidized states. As a result, we extracted the charges from the DFT

calculations and incorporated them into the UFF universal force field.[36] Then we carried out force

field based molecular dynamics (MD) simulations including explicit solvent with anions (PF_6^-) for

several nanoseconds for each of the charge states and each of the ring positions. These calculations

were performed in a box with dimensions of ~ 3.1, ~ 3.1 and 4.1 nm in the x, y and z directions.

The final MD relaxed structures are shown in Figure 5.

Next, we used the 2PT method[37] to calculate the entropy and Gibbs free energy on the basis of the

vibrational modes extracted from the Fourier Transform of the velocity autocorrelation function.

The final free energies (Figure 5) from these MD simulations reveal that the most stable sites are

triazole units, BIPY$^{\bullet+}$ unit and Ar^F rings in the case of the fully oxidized, the radical and the neutral

states, respectively. The results are consistent with the experimental observations. In addition, the

energy barrier for the CBPQT ring to shuttle along the dumbbell component can be estimated by

comparing the differences in free energies for various binding sites: the energy barriers are 21.29

and 7.46 kcal mol^{-1} in the case of the fully oxidized and the neutral states, respectively. These

barriers are in line with the values obtained from dynamic NMR spectroscopy.

Conclusions

We have investigated the shuttling of the CBPQT ring component in a tristable [2]rotaxane in

different oxidation states and demonstrated (Table 1) how this mechanically interlocked molecule

experiences three different kinds of molecular recognition. The reduction of the ring component

from CBPQT^{4+} to CBPQT$^{2(\bullet+)}$ to CBPQT$^{(0)}$ alters its affinity toward the five recognition sites on

the dumbbell components, leading to the ring component preferentially encircling (Figure 6) the

triazole, BIPY$^{\bullet+}$ and Ar^F units, respectively. Significantly, the discovery of stabilizing interactions

between the CBPQT$^{(0)}$ ring and the π-electron-deficient Ar^F units—as experimentally confirmed

by ^{1}H, ^{19}F NMR, UV/Vis/NIR spectroscopies and electrochemical studies, and computationally

proved by DFT based MD calculations—introduces an additional recognition site into CBPQT-

contained rotaxanes. The design of this rotaxane, which demonstrates that an otherwise very weak

interaction between the recognition unit and the ring upon reduction to the fully reduced state can

be enhanced, supports the notion of neighboring component effect and it is more than likely that

this ubiquitous tenet of conformational analysis in the more traditional areas of stereochemistry and physical organic chemistry should surface within the context of presumably other mechanically interlocked molecules.

Associated Content

Supporting information

Detailed synthetic procedures and characterization (HRMS and NMR) data for all compounds, spectroscopic (NMR and UV/Vis/NIR) studies for the rotaxane, X-ray crystallographic analysis data (CIF) for $2 \cdot 2PF_6$, and computational analysis for the rotaxane. This information is available free of charge via the internet at http://pubs.acs.org.

Acknowledgements

References

(1)   Eliel, E. L., *Stereochemistry of Carbon Compounds* McGraw-Hill New York, NY, **1962**.

(2)   Capon, B.; McManus, S. P., *Neighboring Group Participation*. Plenum Press: New York, **1976**; Vol. 1, p 43–75.

(3)   Houminer, Y. *J. Chem. Soc., Perkin Trans. 1* **1975**, 1663–1669.

(4)   Bowden, K. *Chem. Soc. Rev.* **1995**, *24*, 431–435.

(5)   Baasov, T.; Kohen, A. *J. Am. Chem. Soc.* **1995**, *117*, 6165–6174.

(6)   Kanzian, T.; Lakhdar, S.; Mayr, H. *Angew. Chem. Int. Ed.* **2010**, *49*, 9526–9529.

(7)   Maiti, M.; Michielssens, S.; Dyubankova, N.; Maiti, M.; Lescrinier, E.; Ceulemans, A.; Herdewijn, P. *Chem. Eur. J.* **2012**, *18*, 857–868.

(8)   Wang, P.; Tao, W. J.; Sun, X. L.; Liao, S. H.; Tang, Y. *J. Am. Chem. Soc.* **2013**, *135*, 16849–16852.

(9)   Brimioulle, R.; Bach, T. *Science* **2013**, *342*, 840–843.

(10)   Denmark, S. E.; Chi, H. M. *J. Am. Chem. Soc.* **2014**, *136*, 3655–3663.

(11)   Martinez-Cuezva, A.; Lopez-Leonardo, C.; Bautista, D.; Alajarin, M.; Berna, J. *J. Am. Chem. Soc.* **2016**, *138*, 8726–8729.

(12)   Eliel, E. L., *Conformational Analysis*. Interscience Publishers: New York, **1965**.

(13)   Fahrenbach, A. C.; Bruns, C. J.; Cao, D.; Stoddart, J. F. *Acc. Chem. Res.* **2012**, *45*, 1581–1592.

(14)   Fahrenbach, A. C.; Bruns, C. J.; Li, H.; Trabolsi, A.; Coskun, A.; Stoddart, J. F. *Acc. Chem. Res.* **2014**, *47*, 482–493.

(15)   Lehn, J.-M., *Supramolecular Chemistry—Concepts and Perspectives*. Wiley-VCH, Weinheim: **1995**.

(16)   Frasconi, M.; Fernando, I. R.; Wu, Y. L.; Liu, Z. C.; Liu, W. G.; Dyar, S. M.; Barin, G.; Wasielewski, M. R.; Goddard, W. A.; Stoddart, J. F. *J. Am. Chem. Soc.* **2015**, *137*, 11057–11068.

(17)   Trabolsi, A.; Khashab, N.; Fahrenbach, A. C.; Friedman, D. C.; Colvin, M. T.; Coti, K. K.; Benítez, D.; Tkatchouk, E.; Olsen, J.-C.; Belowich, M. E.; Carmielli, R.; Khatib, H. A.; Goddard, W. A., III.; Wasielewski, M. R.; Stoddart, J. F. *Nat. Chem.* **2010**, *2*, 42–49.

18) Fahrenbach, A. C.; Barnes, J. C.; Lanfranchi, D. A.; Li, H.; Coskun, A.; Gassensmith, J. J.; Liu, Z.; Benítez, D.; Trabolsi, A.; Goddard, W. A., III.; Elhabiri, M.; Stoddart, J. F. *J. Am. Chem. Soc.* **2012**, *134*, 3061–3072.

(19) Wang, Y.; Frasconi, M.; Liu, W.-G.; Sun, J.; Wu, Y.; Nassar, M. S.; Botros, Y. Y.; Goddard, W. A., III.; Wasielewski, M. R.; Stoddart, J. F. *ACS. Cent. Sci.* **2016**, *2*, 89–98.

(20) Wang, Y. P.; Frasconi, M.; Stoddart, J. F. *ACS. Cent. Sci.* **2017**, *3*, 927–935.

(21) Wang, Y.; Sun, J.; Liu, Z.; Nassar, M. S.; Botros, Y. Y.; Stoddart, J. F. *Angew. Chem. Int. Ed.* **2016**, *55*, 12387–12392.

(22) Sun, J.; Wu, Y.; Wang, Y.; Liu, Z.; Cheng, C.; Hartlieb, K. J.; Wasielewski, M. R.; Stoddart, J. F. *J. Am. Chem. Soc.* **2015**, *137*, 13484–13487.

(23) Strømgaard, K.; Saito, D. R.; Shindou, H.; Ishii, S.; Shimizu, T.; Nakanishi, K. *J. Med. Chem.* **2002**, *45*, 4038–4046.

(24) Li, H.; Zhu, Z.; Fahrenbach, A. C.; Savoie, B. M.; Ke, C.; Barnes, J. C.; Lei, J.; Zhao, Y.-L.; Lilley, L. M.; Marks, T. J.; Ratner, M. A.; Stoddart, J. F. *J. Am. Chem. Soc.* **2013**, *135*, 456–467.

(25) The minimal energy barrier for the ring component to come across at temperature T is estimated by using the equation $\Delta G^{\ddagger}_c = aT\,[9.972 + \log(T_c/\Delta v)]$, where T_c is the coalescence temperature, $\Delta v = 25$ is the peak separation of proton a and a' in MHz, constant a $= 4.575 \times 10^{-3}$ for units of kcal mol^{-1}. By applying $T = T_c = 343$ K, the minimal energy barrier is calculated as 17.5 kcal mol^{-1}.

(26) Bockman, T. M.; Kochi, J. K. *J. Org. Chem.* **1990**, *55*, 4127–4135.

(27) Because of the close redox potential between the $CoCp_2/CoCp_2^+$ and the $BIPY^{\bullet+}/BIPY^{(0)}$ couple, an excess amount of $CoCp_2$ is needed for the reducing process to reach a higher conversion.

(28)   Mohammad, M. *J. Org. Chem.* **1987**, *52*, 2779–2782.

(29)   Fernando, I. R.; Frasconi, M.; Wu, Y.; Liu, W.-G.; Wasielewski, M. R.; Goddard, W. A.,

III.; Stoddartt, J. F. *J. Am. Chem. Soc.* **2016**, *138*, 10214–10225.

(30)   From the equation $\Delta G^{\ddagger}_c = aT\ [9.972 + \log(T_c / \Delta \nu)]$, one can see that $\log(T_c / \Delta \nu)$ is

considerable compared with 9.972 only when $\Delta \nu$ is small enough. As a result, we take $\Delta \nu = 25$

MHz, i.e., $\Delta \delta = 0.05$ ppm and $T = T_c = 193$ K to calculate the energy barrier, which is 9.6 kcal

mol^{-1}.

(31)   Bin Imran, A.; Esaki, K.; Gotoh, H.; Seki, T.; Ito, K.; Sakai, Y.; Takeoka, Y. *Nat. Commun.*

2014, *5*: 5124.

(32)   Iwaso, K.; Takashima, Y.; Harada, A. *Nat. Chem.* **2016**, *8*, 626–633.

(33)   Zhao, Y.; Truhlar, D. G. *Theor. Chem. Acc.* **2008**, *120*, 215–241.

(34)   Grimme, S.; Antony, J.; Ehrlich, S.; Krieg, H. *J. Chem. Phys.* **2010**, *132*, 154104.

(35)   Frischmann, P. D.; MacLachlan, M. J. *Chem. Soc. Rev.* **2013**, *42*, 871–890.

(36)   Rappe, A. K.; Casewit, C. J.; Colwell, K. S.; Goddard, W. A.; Skiff, W. M. *J. Am. Chem.*

Soc. **1992**, *114*, 10024–10035.

(37)   Pascal, T. A.; Lin, S. T.; Goddard, W. A. *Phy. Chem. Chem. Phy.* **2011**, *13*, 169–181.

Captions to Figures and Scheme

Scheme 1. a) Structural Formula of the [2]Rotaxane 1•6PF$_6$ and Its Graphical Representation, where the Recognition Sites for the Different Redox States of the CBPQT Ring are Shown. b) Synthetic Routes for the Preparation of the Dumbbell 2•2PF$_6$ and the [2]Rotaxane 1•6PF$_6$.

Figure 1. a) Structural formulas of the dumbbell **2**•2PF$_6$ and the [2]rotaxane **1**•6PF$_6$, with the protons and fluorine atoms labelled. b) ^{1}H NMR (500 MHz, CD$_3$CN, 298 K) Spectra of **2**•2PF$_6$ and **1**•6PF$_6$. c) ^{19}F NMR (470 MHz, CD$_3$CN, 298 K) Spectra of **1**•6PF$_6$ and **2**•2PF$_6$. The dashed lines are used to compare the chemical shifts of the signals for the dumbbell **2**•2PF$_6$ with those for the [2]rotaxane **1**•6PF$_6$.
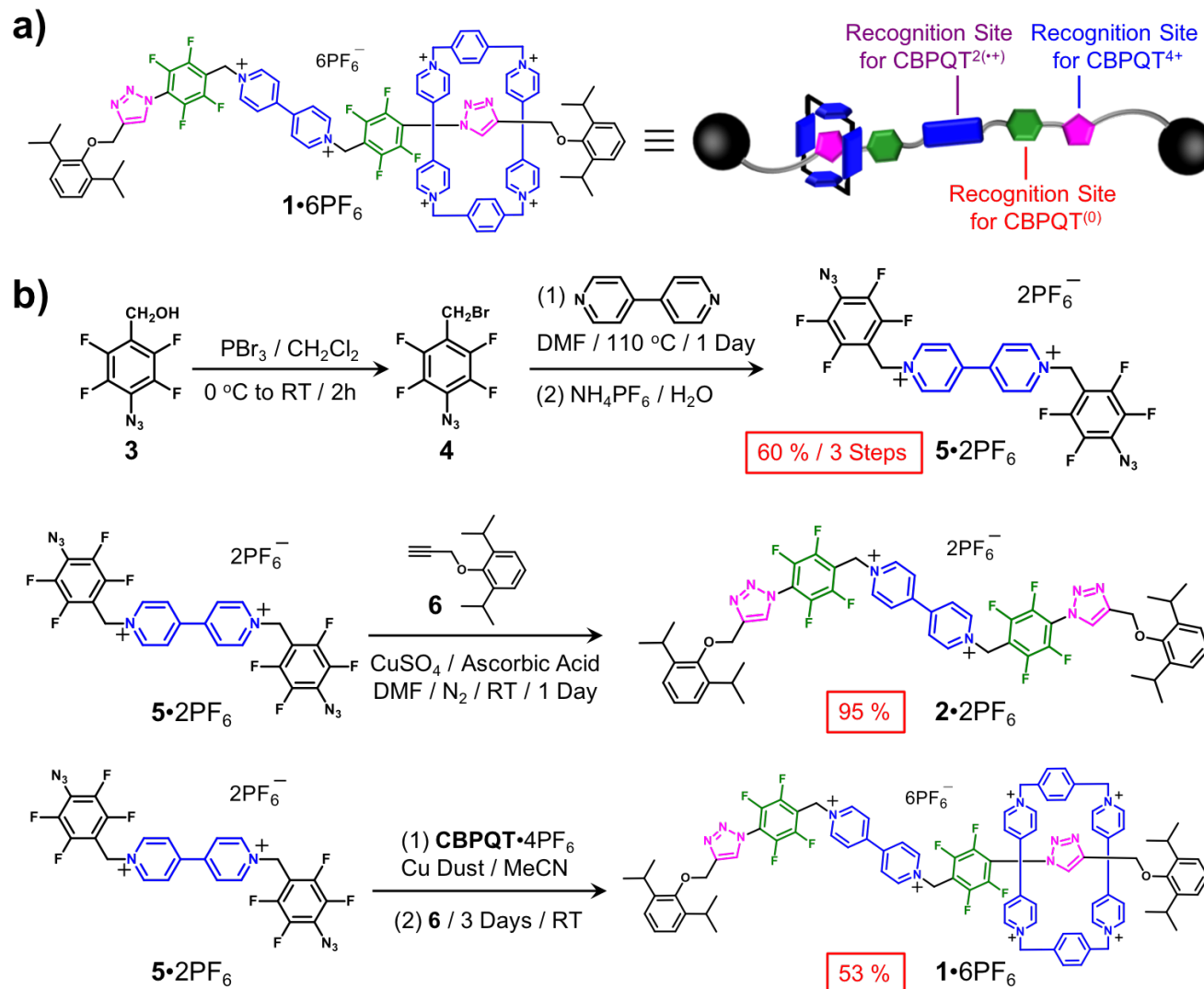
Figure 2. Cyclic voltammograms (CV) of a) **2**$^{2+}$ and b) **1**$^{6+}$. A glassy carbon working electrode, a platinum counter electrode, and an Ag/AgCl reference electrode were used in the characterization of 0.5 mM MeCN solutions of these compounds as their PF$_6^-$ salts at 298 K with 0.1 M TBAPF$_6$ serving as the electrolyte. A scan rate of 200 mV·s^{-1} was used in all the experiments.

Figure 3. a) UV/Vis/NIR Spectra of **2**$^{2+}$ and its reduced forms recorded in MeCN solutions (50 μM) at room temperature. In order to generate **2**$^{(•+)}$ and **2**$^{(0)}$, 1 and 6 equiv of CoCp$_2$ were added, respectively, to MeCN solutions of **2**•2PF$_6$. b) UV/Vis/NIR Spectra of **1**$^{6+}$ and its reduced forms recorded in MeCN solutions (50 μM) at room temperature. In order to generate **1**$^{3(•+)}$ and **1**$^{(0)}$, 3 and 11 equiv of CoCp$_2$ were added, respectively, to MeCN solutions of **1**•6PF$_6$. c) Enlargement of the region between 350 and 650 nm of the spectra in b), showing the strong charge transfer band centered on 550 nm. d) An interpretation of the charge transfer processes that appear in the spectra of **2**$^{(0)}$ and **1**$^{(0)}$.
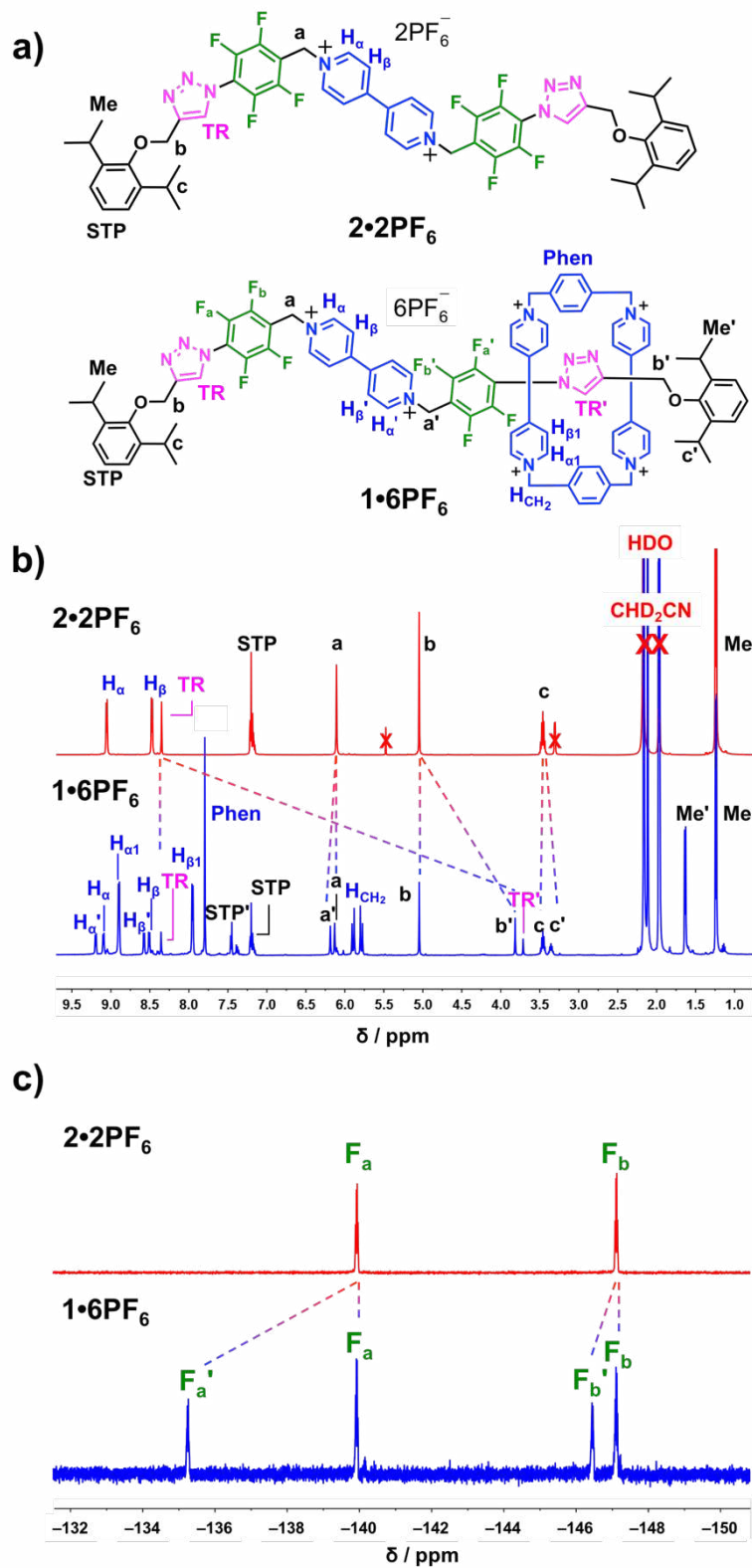
Figure 4. a) Structural formulas of the the dumbbell **2**$^{(0)}$ and the [2]rotaxane **1**$^{(0)}$, with the protons and fluorine atoms labelled. b) ^{1}H NMR (500 MHz, CD$_3$C$_6$D$_5$, 298 K) Spectra of **1**$^{(0)}$ and **2**$^{(0)}$. c) ^{19}F NMR (470 MHz, CD$_3$C$_6$D$_5$, 298 K) Spectra of **1**$^{(0)}$ and **2**$^{(0)}$. The dashed lines are used to compare the chemical shifts of the signals for the dumbbell **2**$^{(0)}$ with those of the [2]rotaxane **1**$^{(0)}$.
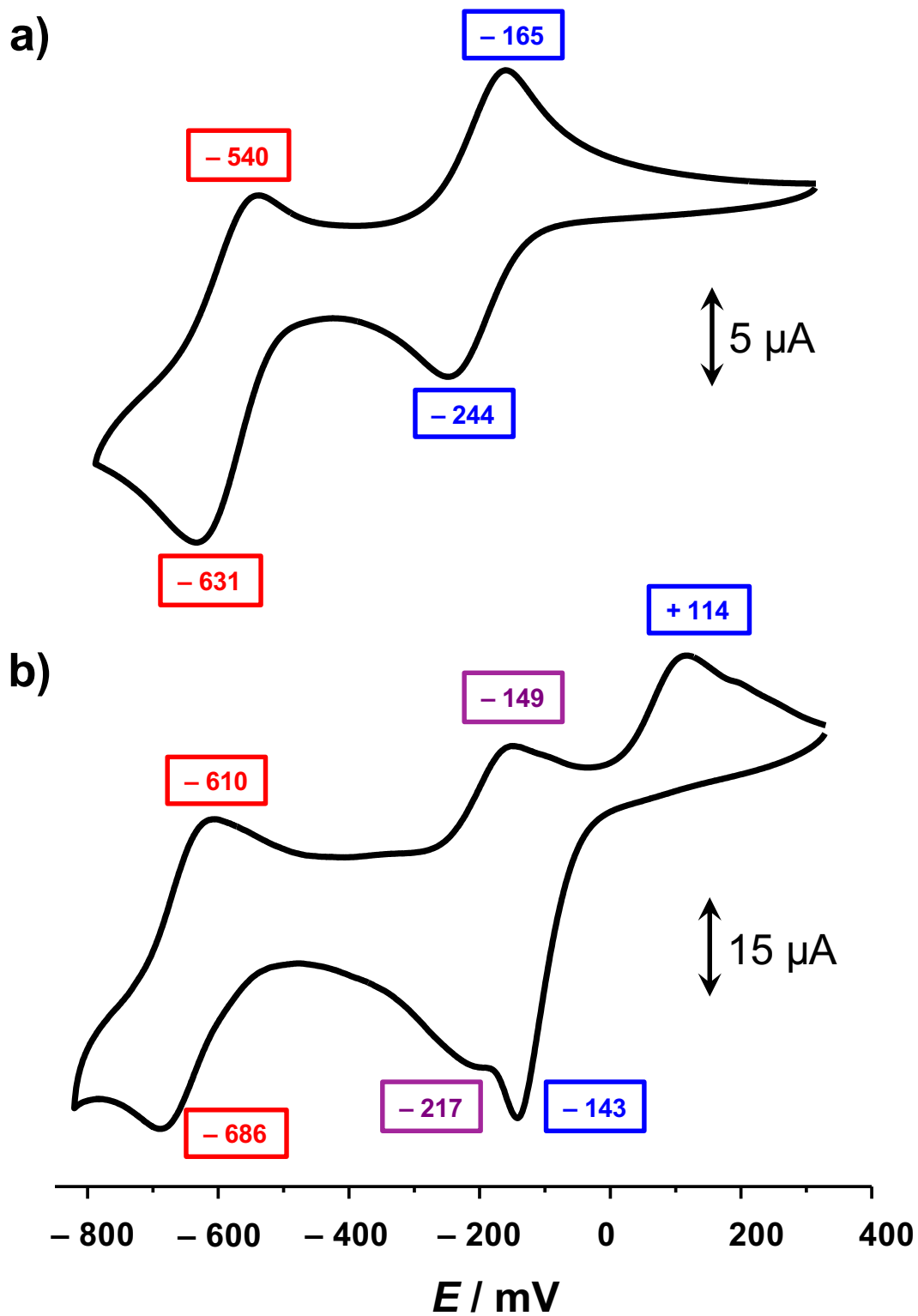
Figure 5. The simulated co-conformations of the [2]rotaxane at different oxidation states and their relative energy level. In each oxidation state, the energy of the most stable co-conformation is assigned to be 0 kcal mol^{-1}.
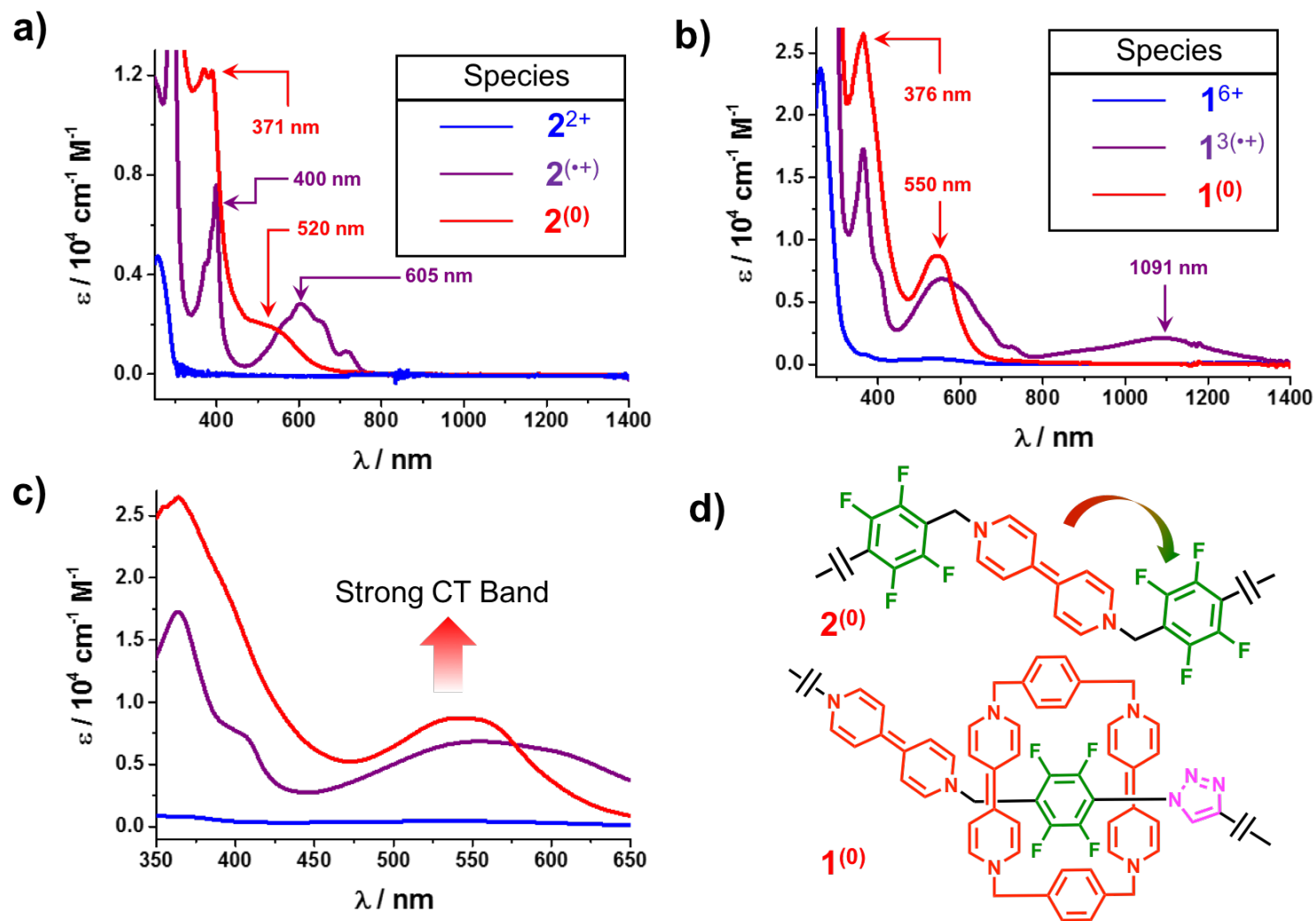
Figure 6. A graphical summary of the actuating processes with the energy levels involved in the [2]rotaxane as a result of changes in its redox state. a) In the fully oxidized state, the CBPQT^{4+} ring encircles the triazole unit and does not shuttle along the dumbbell component on either the ^{1}H or the ^{19}F NMR timescales. In the radical state, the CBPQT$^{2(•+)}$ ring interacts with the BIPY$^{•+}$ unit and gives rise to the formation of a trisradical tricationic species. In the neutral state, the CBPQT$^{(0)}$ ring recognizes the electron-deficient Ar^F recognition sites, forming a charge transfer complex. The ring shuttles quickly along the dumbbell component because of the removal of the Coulombic repulsion present in the fully oxidized state. b) The energy profiles for the [2]rotaxane in different redox states when the ring shuttles along the dumbbell component. The lines in pink, blue, purple, red and green correspond to the recognition units shown in a).
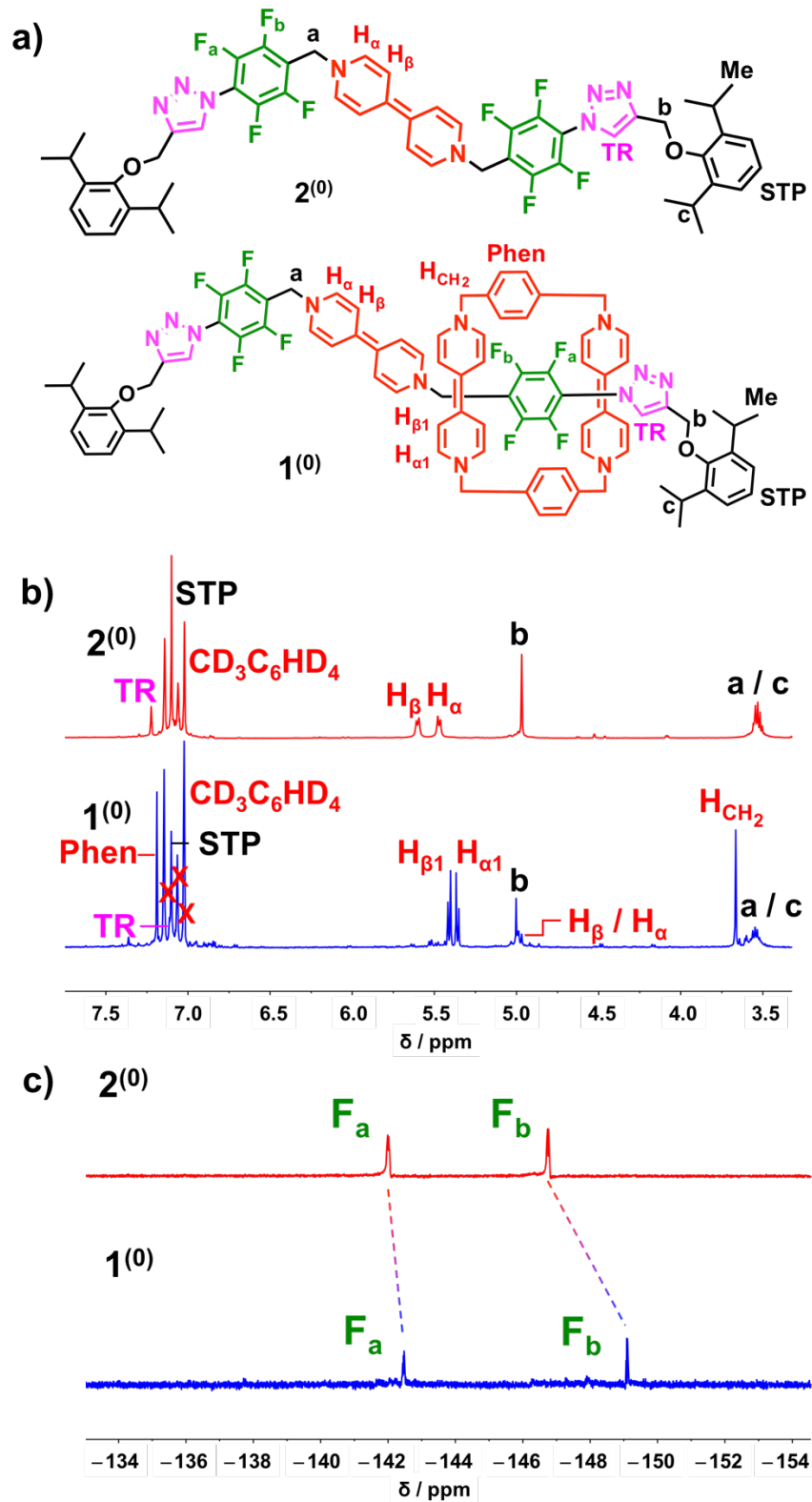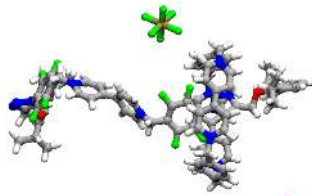
a)

1·6PF₆

Recognition Site for CBPQT²(•⁺)

Recognition Site for CBPQT⁴⁺

Recognition Site for CBPQT⁽⁰⁾

b)

3 → PBr₃ / CH₂Cl₂, 0 °C to RT / 2h → **4**

(1) 4,4'-bipyridine, DMF / 110 °C / 1 Day
(2) NH₄PF₆ / H₂O

60 % / 3 Steps **5·2PF₆**

5·2PF₆ + **6** → CuSO₄ / Ascorbic Acid, DMF / N₂ / RT / 1 Day → 95 % **2·2PF₆**

5·2PF₆ → (1) **CBPQT·4PF₆**, Cu Dust / MeCN (2) **6** / 3 Days / RT → 53 % **1·6PF₆**

Scheme 1

Figure 1

Figure 2

Figure 3

Figure 4
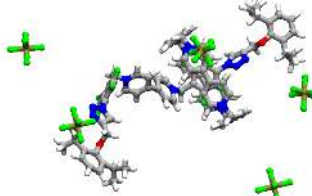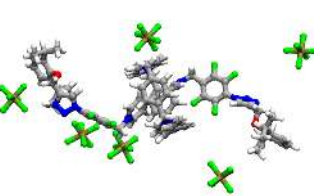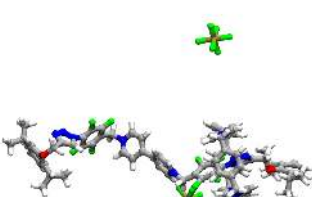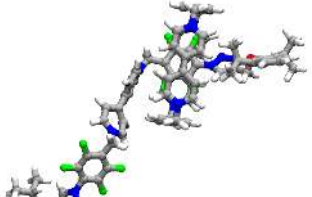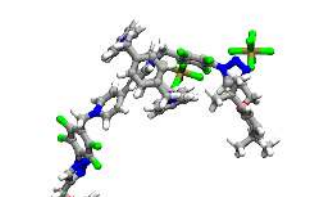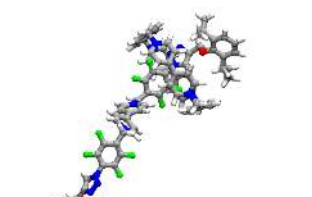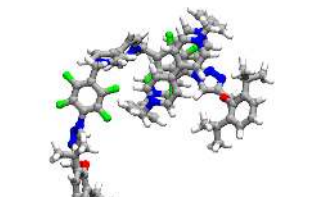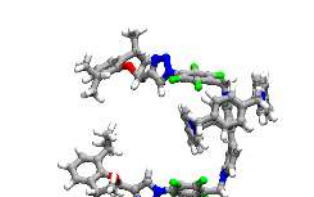
Redox State	Triazole unit	Ar^F ring	BIPY$^{•+}$ unit
6+			
ΔG (kcal mol^{-1})	0.00	21.29	19.86
3(•+)			
ΔG (kcal mol^{-1})	1.22	10.75	0.00
0			
ΔG (kcal mol^{-1})	12.21	0.00	7.46

Figure 5

a)

$\Delta G^{\ddagger}_{c} \geq 17.5$ kcal mol^{-1}

4+   2+   2+   4+

$\rightleftharpoons$X$\rightleftharpoons$

Electrostatic Barrier

3e$^-$ 3e$^-$

3+3•

3e$^-$ 3e$^-$

Radical-Pairing Interactions

$\Delta G^{\ddagger}_{c} \leq 9.6$ kcal / mol^{-1}

Charge Transfer Interactions

b)

Energy   **Oxidized State**

$\Delta G^{\ddagger}_{c} \geq 17.5$ kcal mol^{-1} Ring Position

Energy   **Reduced State**

Ring Position

Energy   **Neutral State**

$\Delta G^{\ddagger}_{c} \leq 9.6$ kcal mol^{-1}
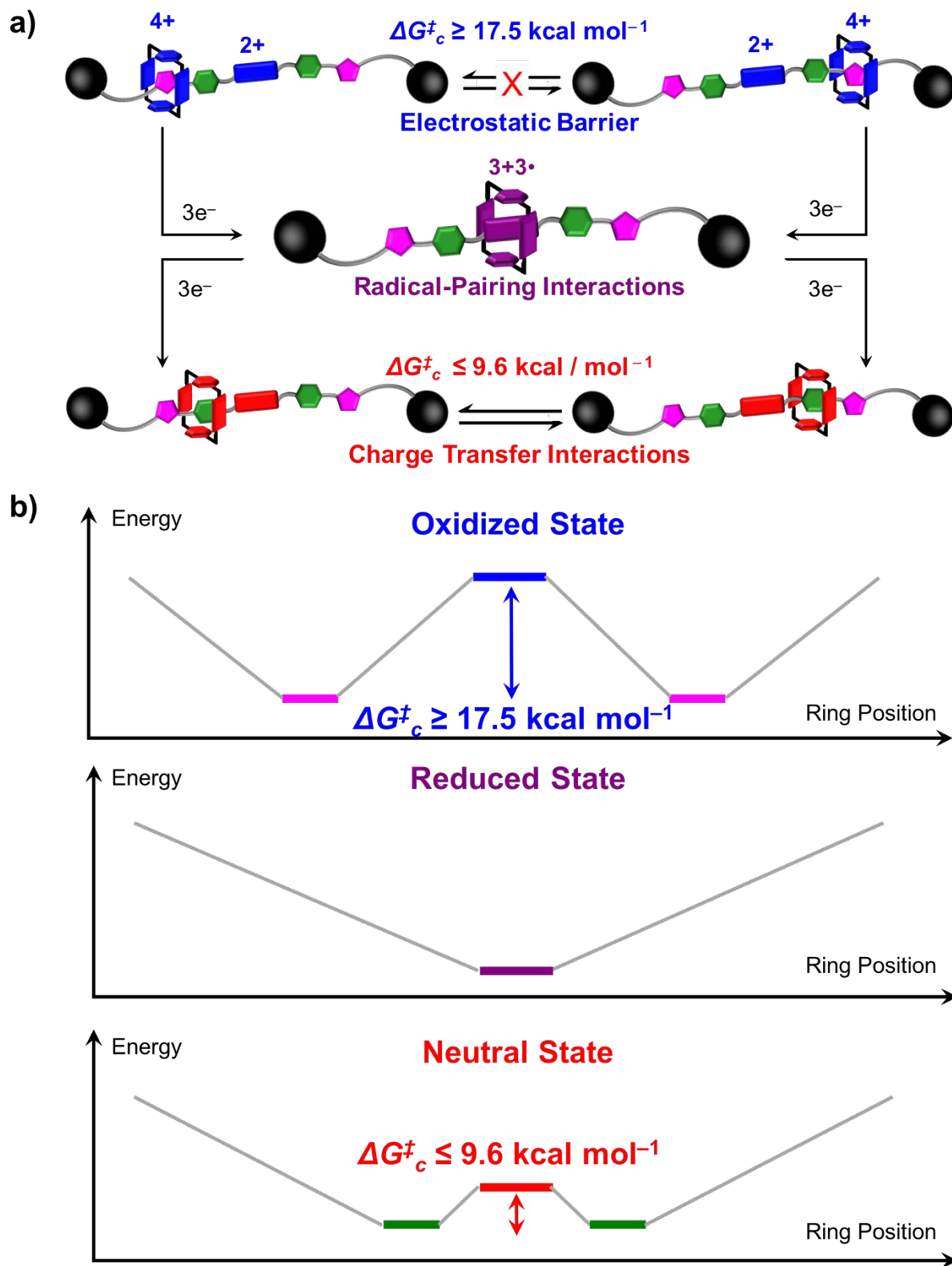
Ring Position

Figure 6

Table 1. Summary of the Key Spectral Features of the [2]Rotaxane in Its Different Oxidation States, in Comparison with Those of the Dumbbell Compound, which Reveals the Interactions between the CBPQT Ring and the Corresponding Recognition Site(s).

Oxidation State of the [2]Rotaxane	Recognition Site(s)	Key Spectral Features of the [2]Rotaxane	Corresponding Spectral Features of the Dumbbell
6+	Triazole rings	$\delta(H_{TR}') = 3.72$ ppm $\delta(H_a') = 6.21$ ppm $\delta(F_a') = -135.3$ ppm	$\delta(H_{TR}) = 8.36$ ppm $\delta(H_a) = 6.16$ ppm $\delta(F_a) = -140.0$ ppm
$3(\bullet+)$	$BIPY^{\bullet+}$ unit	Reduction potentials at -143 and -217 mV UV/Vis/NIR absorption band at 1091 nm	Reduction potential at -244 mV UV/Vis/NIR absorption bands at 400 and 605 nm
0	Ar^F units	Strong UV/Vis/NIR absorption bands at 376 and 550 nm Reduction potential at -686 mV $\delta(F_b) = -149.1$ ppm	Weak UV/Vis/NIR absorption bands at 371 and 520 nm Reduction potential at -631 mV $\delta(F_b) = -146.7$ ppm

TOC Graphic

Mechanical Bond-Induced
Neighboring Component Effect